

Conserved High Activity Binding Peptides are Involved in Adhesion of Two Detergent-Resistant Membrane-Associated Merozoite Proteins to Red Blood Cells during Invasion

Ana Zuleima Obando-Martinez,^{†,‡} Hernando Curtidor,^{†,‡} Gabriela Arévalo-Pinzón,^{†,‡} Magnolia Vanegas,^{†,‡} Carolina Vizcaino,^{†,‡} Manuel Alfonso Patarroyo,^{†,‡} and Manuel Elkin Patarroyo^{*,†,§}

[†]Fundación Instituto de Inmunología de Colombia, Carrera 50 No. 26-20, Bogotá, Colombia, [‡]Universidad del Rosario, Calle 14 No. 6-25, Bogotá, Colombia, and [§]Universidad Nacional de Colombia, Carrera 45 No. 26-85, Bogotá, Colombia

Received October 5, 2009

Detergent resistant membranes (DRMs) of *Plasmodium falciparum* merozoites contain a large number of glycosylphosphatidylinositol (GPI)-anchored proteins that have been implicated in interactions between merozoites and red blood cells (RBCs). In this study, two cysteine-rich proteins anchored by GPI to merozoite DRMs (Pf92 and Pf113) were studied with the aim of identifying regions actively involved in RBC invasion. By means of binding assays, high-activity binding peptides (HABPs) with a large number of binding sites per RBC were identified in Pf92 and Pf113. The nature of the RBC surface receptors for these HABPs was explored using enzyme-treated RBCs and cross-linking assays. Invasion inhibition and immunofluorescence localization studies suggest that Pf92 and Pf113 are involved in RBC invasion and that their adhesion to RBCs is mediated by such HABPs. Additionally, polymorphism and circular dichroism studies support their inclusion in further studies to design components of an antimalarial vaccine.

Introduction

Detergent resistant membranes (DRMs^a) or lipid rafts are specialized membrane microdomains formed by tightly associated proteins, cholesterol, and sphingolipids, which are found in the cell-membrane bilayers of almost all organisms, including mammals, protozoan, bacteria, and viruses.^{1–3} The high content of saturated hydrocarbon chains in DRM sphingolipids and phospholipids favors the formation of highly ordered membrane platforms, whereas the unsaturated hydrocarbons of phospholipids from the surrounding membrane bilayer form a liquid-disordered phase.^{4,5}

DRM proteins have been implicated in a significant number of critical cellular processes, such as signal transduction,

cytoadherence, lipid trafficking, cell polarization, and cellular movement.^{4,6,7} In *Plasmodium falciparum*, the protozoan parasite responsible for the most severe form of human malaria, DRMs have been suggested to provide a site for protein–protein interactions between the red blood cell (RBC) and the merozoite (parasite stage that invades RBCs), which are a crucial step for the development of the asexual intraerythrocytic cycle and hence for the pathogenesis and symptoms of malaria.^{8–10}

Malaria is one of the most challenging problems for public health systems worldwide because of the heavy burden of disease and death it imposes to people living in endemic areas.¹¹ All attempts to control the spread of this lethal disease have been largely hindered by the emergence of drug-resistant parasite strains and insecticide-resistant mosquito vectors,¹² therefore leaving vaccine development as one of the long-term fully effective alternatives to tackle this problem. With such purpose in mind, a large body of research has focused on the identification of potential vaccine targets in *P. falciparum* proteins implicated in the invasion process.^{8,10,13,14}

For instance, merozoite surface proteins participate in receptor–ligand interactions occurring during the parasite's initial attachment to RBCs, rolling over RBC surface, reorientation, and entry into RBCs. Among these proteins are included glycosylphosphatidylinositol (GPI)-anchored merozoite surface proteins (MSPs) (MSP1, -2, -4, -5, -10), soluble MSPs (MSP3, -6, -7, -9/acid basic repeat antigen (ABRA), and -11), and others such as Pf12, Pf38, Pf41, serine repeat antigen-5 (SERA-5), and the apical merozoite antigen-1 (AMA-1).^{9,15,16} Soluble proteins have been described to associate with GPI-anchored DRM proteins to form coligand complexes that interact with receptors of the RBC surface (a scheme of such lipid platform complexes is shown in Figure 1).^{14,17,18}

*To whom correspondence should be addressed. Address: Fundación Instituto de Inmunología de Colombia, Carrera 50 No. 26-20, Bogotá, Colombia. Phone: +57-1-3244672, extension 146. Fax: +57-1-3244672/73, extension 108. E-mail: mepatarr@mail.com.

^a Abbreviations: AMA-1, apical merozoite antigen-1; BS³, bis-sulfosuccinimidyl suberate; CD, circular dichroism; DBL, Duffy-binding-like; DRM, detergent resistant membrane; EGF-like, epidermal-growth-factor-like; EGTA, ethylene glycol tetraacetic acid; ELISA, enzyme-linked immunosorbent assay; FBS, fetal bovine serum; gDNA, genomic DNA; GFP, green fluorescent protein; GPI-anchor, glycosylphosphatidylinositol–anchor; HABP, high activity binding peptide; HBS, HEPES buffered saline; HEPES, 4-(2-hydroxyethyl)-1-piperazineethanesulfonic acid; HLAs, human leukocyte antigens; IFA, indirect immunofluorescence assay; K_d, dissociation constant; m-, peptide mixture; MAAP, malarial adhesins and adhesin-like proteins predictor; MALDI-ToF MS, matrix assisted laser desorption/ionization time-of-flight mass spectrometry; MHC II, major histocompatibility complex class II; MSP, merozoite surface protein; n_H, Hill coefficient; PBS, phosphate buffered saline; Pfs48/45, sexual stage antigen; RBC, red blood cell; RP-HPLC, reverse phase-high performance liquid chromatography; SDS–PAGE, sodium dodecyl sulfate polyacrylamide gel electrophoresis; SERA-5, serine repeat antigen-5; Sites/cell, binding sites per RBC; *t*-Boc, *tert*-butyloxycarbonyl; TBS–T, tris-buffered saline–0.05% Tween; TCR, T-cell receptor.

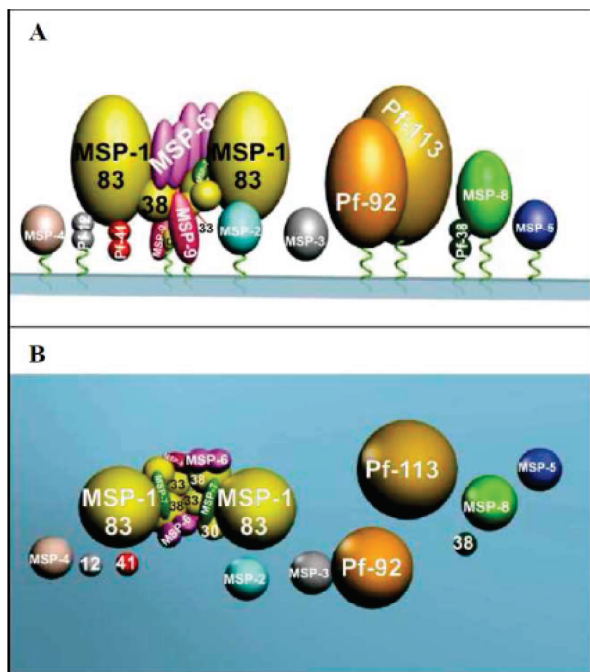


Figure 1. Schematic representation of detergent resistant lipid raft-like membrane-associated proteins showing some of the protein complexes reported to date (coligand complexes). Molecules are drawn at their approximate molecular weight. The top panel (A) shows the lateral view of the hypothetical organization of these proteins, while the bottom panel (B) corresponds to a top view. GPI anchors are depicted as green twists traversing the pale-blue membrane. As indicated in the figure, no proteins are known to be associated with Pf92 and Pf113. This figure is reprinted from *Vaccine* (<http://www.sciencedirect.com/science/journal/0264410X>), Vol. 26, Pinzon, C. G.; Curtidor, H.; Bermudez, A.; Forero, M.; Vanegas, M.; Rodriguez, J.; Patarroyo, M. E., Studies of *Plasmodium falciparum* Rhoptry-Associated Membrane Antigen (RAMA) Protein Peptides Specifically Binding to Human RBC, pages 853–862, Copyright 2009, with permission from Elsevier.⁵⁷

Among these GPI-anchored molecules, adhesion proteins containing Pfs48/45 domains formed by six conserved cysteines (therefore denoted as Cys₆ proteins) have been largely studied as potential candidate targets for blocking the development of parasite asexual stages inside the *Anopheles* mosquito.¹⁹ These proteins are located on the gametocyte surface where they appear to be implicated in gamete fertilization and cellular adhesion.²⁰ Interestingly, two Cys₆ GPI-anchored proteins, named Pf12 and Pf38, are also expressed by the merozoite during the intraerythrocytic developmental stage, whereas another Cys₆ protein not anchored by GPI and named Pf41 is expressed only during the merozoite stage but not during gametocyte stages.⁸ Additionally, Pf12, Pf38, and Pf41 have been proposed to be involved in merozoite adhesion to RBCs during the invasion process,^{8,14,21} therefore increasing the interest in studying other Cys₆ proteins as well as proteins with similar features.

Pf92 and Pf113 are two components of DRMs that, same as Pf12, Pf38, and Pf41, contain cysteine-rich domains despite not sharing high homology with these three proteins.^{8,14} Both proteins are anchored to the parasite membrane by GPI and contain a signal peptide, as expected of surface proteins.^{8,22} Pf92 is expressed during merozoite stages and contains a Pfs48/45 domain at its C-terminus (Figure 2A), which is very similar to the domains of Cys₆ proteins except that it only contains four cysteine residues. On the other hand, transcriptome studies

describe Pf113 as a putative protein expressed during ring, sporozoite, and merozoite stages,²³ but immunofluorescence studies with Pf113-green fluorescent protein (GFP) fusion constructs have not yet been carried out to determine whether this protein is indeed localized in merozoite surface.⁸ However, the malarial adhesins and adhesin-like proteins predictor (MAAP) classifies Pf113 as an adhesin²⁴ together with other well-characterized GPI-anchored RBC binding proteins like MSP1, MSP2, and MSP10. These features suggest a potential role of Pf92 and Pf113 in RBC invasion, possibly by mediating adhesion of merozoites to RBCs via receptor–ligand interactions.

Interestingly, a previous robust receptor–ligand study performed with the Cys₆ proteins Pf12, Pf38, and Pf41 led to the identification of amino acid sequences with the ability to establish high affinity and specific molecular interactions with RBC receptors, therefore being designated as high activity binding peptides (HABPs).²¹ Such a study proposed a correlation between the adhesive function of these Cys₆ proteins and the loops formed by disulfide bonds linking conserved cysteines, given that one HABP of Pf12, Pf38, and Pf41 was identified inside a similar loop in each of these proteins. In Pf92, the Pfs48/45 domain contains loops comparable to the ones described in Pf12, Pf38, and Pf41, whereas Pf113 does not contain a Pfs48/45 domain and hence has not been proposed to form similar loops. No cell adhesion regions have been described in these two proteins to date.

In this study, the entire sequences of Pf92 and Pf113 were synthesized as 20-mer-long, nonoverlapping peptides and assessed using a highly sensitive and specific receptor–ligand assay previously described by us,^{16,25,26} which enables the identification of amino acid sequences with high specific binding activity to target cells, thereby denoted as Pf92 and Pf113 HABPs. These HABPs showed well-defined secondary structure elements and high conservation among different *P. falciparum* strains according to our polymorphism studies. The binding constants of all Pf92 and Pf113 HABPs were determined by performing saturation assays. Binding profiles of HABPs to enzyme-treated RBCs as well as cross-linking patterns to RBC surface proteins were obtained in order to elucidate the nature of the possible RBC receptor(s). Moreover, invasion inhibition assays were carried out with HABPs and sera raised against Pf92/Pf113 peptides to examine their possible involvement in RBC invasion. The same anti-Pf92/Pf113 sera were used to test the localization of both proteins by indirect immunofluorescence assays (IFA).

Our findings suggest that binding of these adhesion proteins to RBC receptors is mediated by HABPs, which supports including the HABPs identified in this study as possible targets for developing a fully effective subunit-based, multi-epitopic, multistage, chemically synthesized antimalarial vaccine. It would be necessary for that purpose to determine whether these HABPs can induce a protective response and use their sequences as template to design HABP analogues capable of forming a more stable major histocompatibility complex class II (MHC II)-peptide-T-cell receptor (TCR) complex. Such improved immunogenic peptides could eventually be used as vaccine components as has been reported previously by us.²⁷

Results

Identification of High Activity Binding Peptides in Pf92 and Pf113. Receptor–ligand assays performed with Pf92- and

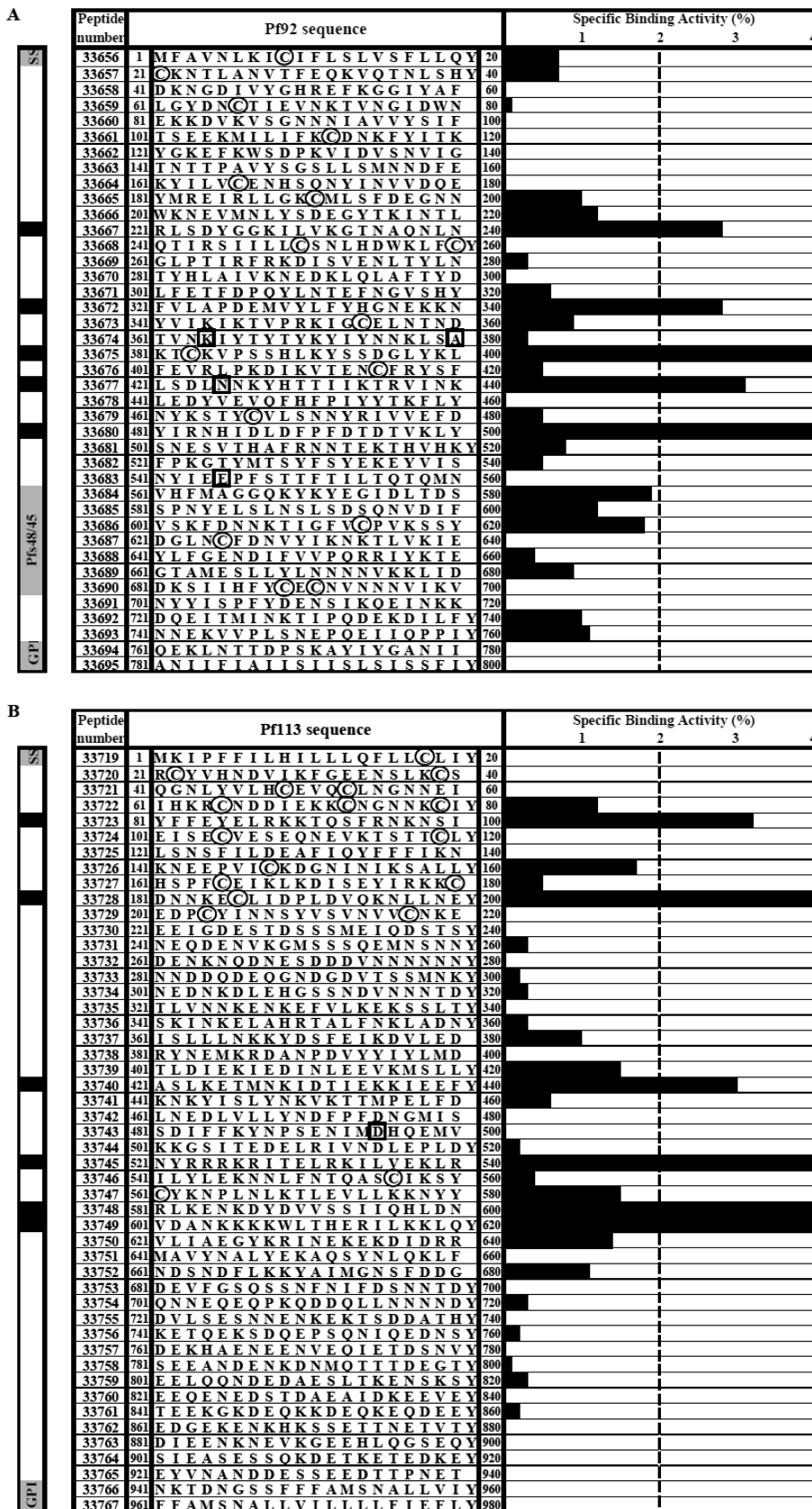


Figure 2. Binding profile of (A) Pf92 peptides and (B) Pf113 peptides as determined by binding assays with human RBCs. Specific binding activities are represented by the length of the horizontal black bars shown in front of each peptide sequence. The vertical bars shown to the left are schematic representations of Pf92 and Pf113, where the localizations of the signal sequence (SS), GPI anchor (GPI), the Pfs48/45 domain present in members of the Cys₆ protein family, and HABPs (black boxes) are indicated. Cysteines are enclosed by black circles, and the polymorphic amino acid positions found in this study are shown enclosed inside black boxes.

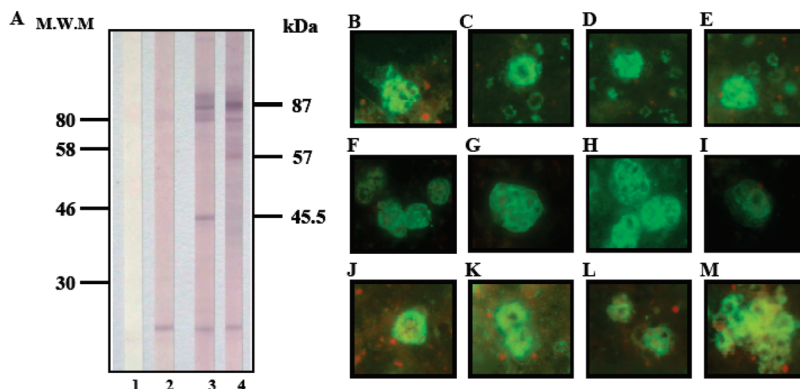


Figure 3. Assessment of anti-Pf92 and anti-Pf113 rabbit sera with parasite lysate and late schizonts. (A) Western blot analysis of late schizont lysate incubated with anti-Pf92 rabbit sera. Lanes 1 and 2 correspond to preimmune sera from two rabbits inoculated with a mixture of Pf92 peptides 33660, 33684, and 33691. Lanes 3 and 4 correspond to immune sera from the same rabbits. M.W.M indicates molecular weight marker. Fixed and blocked late schizonts and ring stages were incubated with rabbit anti-Pf92 immune sera (B–I) or with Pf113 immune rabbit sera (J–M). Immunofluorescence with preimmune serum from each rabbit showed no detection of any protein in the schizont and ring stages (data not shown).

Pf113-radiolabeled peptides identified Pf92 peptides 33667, 33672, 33675, 33677, and 33680, as well as Pf113 peptides 33723, 33728, 33740, 33745, 33748, and 33749 as HABPs, given that these 20-mer-long nonoverlapping peptides bound specifically to RBC receptors with binding activities greater than 2.0% (>2.5% for all Pf92 and Pf113 HABPs as indicated by the length of the black horizontal bar shown in front of each peptide's amino acid sequence in Figure 2, in all cases larger than the dotted vertical line).

Pf92 HABPs were localized in the protein's central region, which contains a large number of Cys residues (shown encircled in Figure 2), but no HABPs were located inside the loops of the Pfs48/45 domain (Figure 2A) where one HABP was previously identified for Pf12, Pf38, and Pf41.²¹ Similarly, as shown in Figure 2B, two Pf113 HABPs (33723 and 33728) were located at the Cys-rich N-terminal region. The other four Pf113 HABPs (33740, 33745, 33748, and 33749) were located in the protein's central region near two Cys residues that are likely to form a disulfide bridge.

Scrambled-sequence peptides synthesized on the basis of the amino acid compositions of Pf92 HABPs (33667 and 33675) and Pf113 HABPs (33723 and 33740) showed specific binding activities much lower than the ones of their corresponding original HABPs (Figure S1). All scrambled peptides had binding activities below 2.0%, thus indicating that specific binding of HABPs to RBCs depends on the specific amino acid sequence rather than the amino acid composition and shows the specificity of the methodology used in the identification of HABPs.

Proteins in Merozoite Lysate are Recognized by Rabbit Sera. The Western blot analysis of late-schizont lysate with sera raised by inoculating rabbits with a peptide mixture containing Pf92 peptides 33660, 33684, 33691 and the T-helper cell determinant FIS peptide²⁸ (m-2 mixture) recognized three bands with apparent molecular weights of 45.5, 57, and 87 kDa (Figure 3A, lanes 3 and 4) that were not detected by rabbits' preimmune sera (Figure 3A, lanes 1 and 2). This suggests the specific recognition of Pf92, which probably corresponds to the 87 kDa band considering that it has been repeatedly reported that the apparent molecular weights of some *P. falciparum* proteins differ from their predicted weights.²⁹ The other two bands probably correspond to cleavage fragments of Pf92 containing sequences

that are also recognized by these rabbits' sera. On the contrary, no proteins were recognized by sera raised against the m-1 mixture consisting of Pf92 HABPs 33667, 33672 and FIS peptide (data not shown).

Sera obtained by immunizing rabbits with the m-3 mixture (Pf113 HABPs 33723, 33728 and FIS) showed a slight recognition of a 119 kDa band close to the molecular weight of Pf113 and two apparent cleavage fragments of about 25 and 29 kDa (data not shown). No bands were detected by sera raised against the m-4 mixture (Pf113 peptides 33733, 33754, 33765 and FIS) in the Western blot analysis of *P. falciparum* late schizonts. Sera from rabbits receiving only the FIS peptide showed no recognition of any parasite protein in schizont lysate (data not shown).

Localization of Pf92 and Pf113 in Intraerythrocytic Parasite Stages. The results of immunofluorescence assays with *P. falciparum* late schizonts localized Pf92 in merozoite surface (Figure 3, panels B–I), which is consistent with the fluorescence pattern reported for the Pf92-GFP fusion protein⁸ but also showed the presence of this protein in ring stages (Figure 3, panels C–E). Conversely, Pf113 was only detected on the merozoite surface, and not in other sub-cellular compartments or in any other intraerythrocytic life-cycle stage (Figure 3, panels J–M). Sera from rabbits inoculated only with FIS showed no recognition of any protein in *P. falciparum* schizonts or ring stages (data not shown).

Determination of Antibody Titers in Rabbits' Sera by Enzyme-Linked Immunosorbent Assay (ELISA). The rabbit's sera that recognized proteins in schizont lysate by Western blot and native proteins by IFA (i.e., anti-m-2 and anti-m-3 sera raised against Pf92 and Pf113, respectively) had high antibody titers against each of the peptides included in such peptide mixtures except against peptide 33660 included in m-2, as shown in Table 3.

Saturation of RBC Receptors Sites with Pf92 and Pf113 HABPs. Saturation plots were obtained for each Pf92 and Pf113 HABP to determine dissociation constants (K_d), Hill coefficients (n_H), and the number of receptors sites per RBC. As shown in Figure 4 and Table 1, there was a tendency for HABPs to saturate their binding sites on RBCs. Also, all HABPs had different binding affinities and a different number of binding sites per RBC, even among HABPs belonging to the same protein.

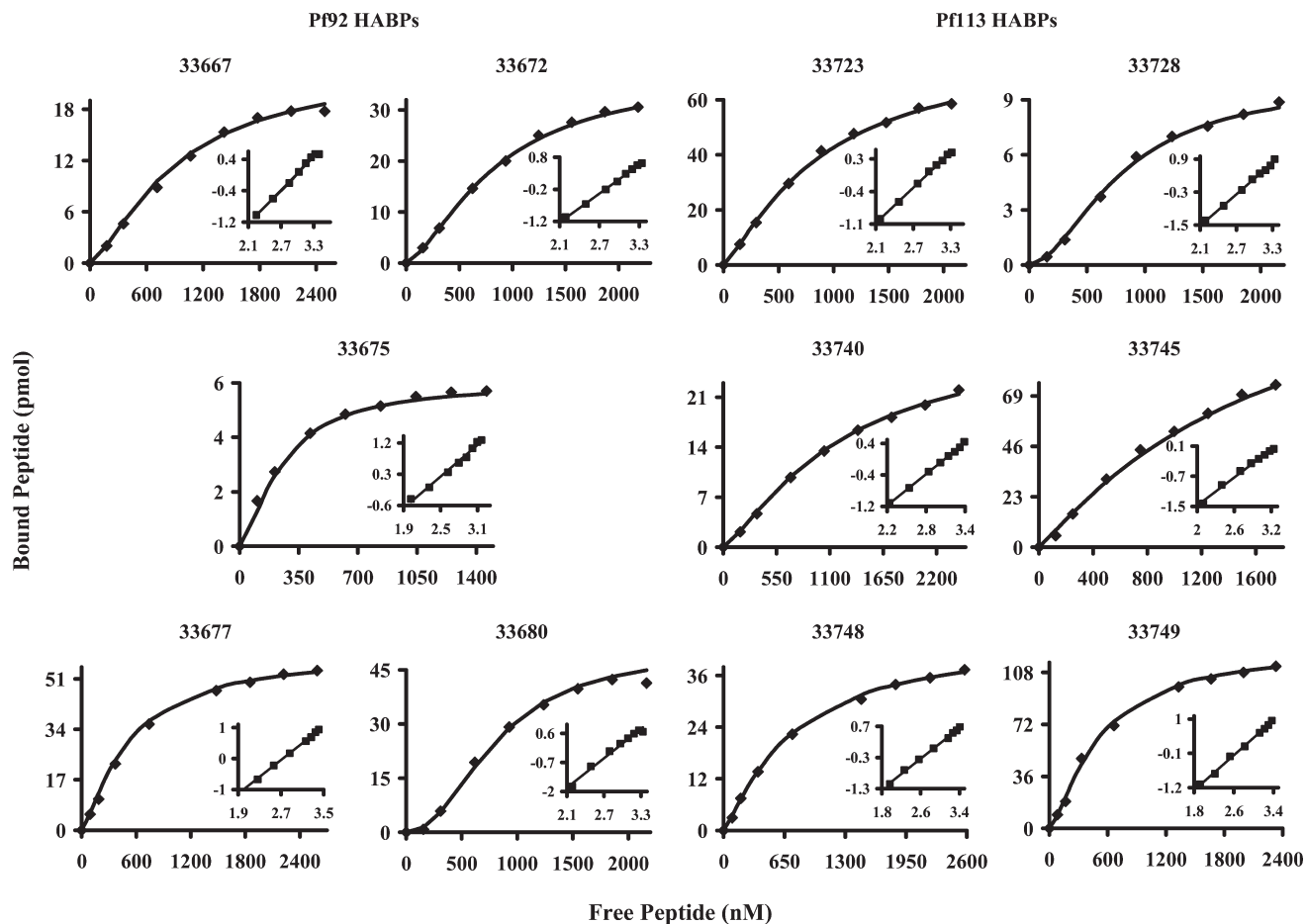


Figure 4. Saturation assays with Pf92 and Pf113 HABPs. The curves represent specific binding. In the Hill plot (inset), the x-axis corresponds to $\log F =$ free peptide and the y-axis to $\log(B/B_{\max} - B)$, where B is the amount of bound peptide and B_{\max} the maximum amount of bound peptide.

Table 1. Binding Constants of Pf92 and Pf113 HABPs obtained from Saturation Curves

HABP	K_d (nM) ^a	n_H ^b	Sites/cell ^c
Pf92			
33667	900	1.4	184700
33672	850	1.5	305200
33675	250	1.5	48200
33677	520	1.3	481800
33680	800	2.2	200700
Pf113			
33723	900	1.3	642400
33728	800	1.9	80300
33740	1200	1.3	240900
33745	1700	1.1	1164400
33748	730	1.2	361400
33749	510	1.4	1003800

^aDissociation constants. ^bHill coefficients. ^cBinding sites per RBC.

In general, the majority of Pf92 and Pf113 HABPs showed high binding affinities with nanomolar dissociation constants. All Pf92 HABPs established binding interactions of cooperative nature with RBC membrane receptors, as indicated by their Hill coefficients larger than 1.3, with HABP 33680 showing the largest coefficient ($n_H = 2.2$). Pf113 HABPs also established binding interactions of positive cooperativity with Hill coefficients slightly smaller than the ones shown by Pf92 HABPs ($n_H > 1.1$), with HABP 33728

Table 2. Percentages of Specific Binding to Enzyme-Treated RBCs^a

HABP	control (%)	neuraminidase (%)	chymotrypsin (%)	trypsin (%)
Pf92				
33667	100	67	79	11
33672	100	5	116	31
33675	100	23	37	55
33677	100	30	124	16
33680	100	120	90	29
Pf113				
33723	100	17	31	83
33728	100	13	59	105
33740	100	12	33	87
33745	100	68	7	43
33748	100	55	94	18
33749	100	25	87	50

^aStandard deviations were below 5%.

showing the highest coefficient ($n_H = 1.9$). This suggests that binding of native Pf92 and Pf113 proteins to RBC membrane receptors by means of HABPs favors binding of other copies of the same protein.

Enzymatic Treatment. Binding assays were carried out to evaluate the specific binding of Pf92 and Pf113 HABPs to RBCs treated enzymatically with chymotrypsin, trypsin, or neuraminidase (Table 2). Specific binding of Pf92 HABPs 33672 and 33677 as well as of Pf113 HABPs 33748 and 33749

was significantly reduced by treating RBCs with neuraminidase and trypsin ($\geq 45\%$). On the other hand, neuraminidase and chymotrypsin reduced binding of Pf113 HABPs 33723, 33728, and 33740 and Pf92 HABP 33675 by more than 50%. The binding of this latter HABP was also reduced significantly by treatment with trypsin ($>45\%$).

Binding of Pf92 HABP 33680 was predominantly reduced by treating RBCs with trypsin (29% specific binding), whereas a slight reduction was observed upon treating RBCs with chymotrypsin (90% specific binding). Binding of Pf92

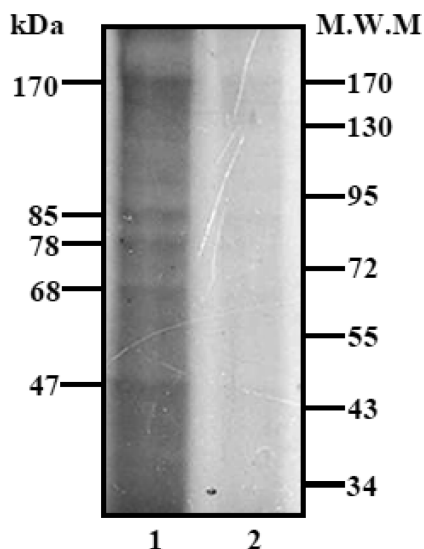


Figure 5. Autoradiogram of the RBC surface receptors cross-linked by Pf92 HABP 33680: (lane 1) total binding; (lane 2) unspecific binding. Bands of ~ 85 and ~ 78 kDa were also cross-linked by all Pf113 HABPs. M.W.M indicates molecular weight marker.

HABP 33667 was drastically reduced by trypsin and in a lesser proportion by neuraminidase and chymotrypsin. All enzymatic treatments reduced binding of Pf113 HABP 33745, but such reduction was more drastic when RBCs were treated with chymotrypsin and trypsin (specific binding was below 50% in both cases), whereas treatment with neuraminidase reduced specific binding of this HABP to 68% (Table 2).

Approximation to the Molecular Weights of the RBC Receptors for Pf92 and Pf113 HABPs. Cross-linking assays for some HABPs of Pf92 and Pf113 were carried out under total binding (radiolabeled peptide) and unspecific binding (radiolabeled peptide with an excess of nonradiolabeled peptide) conditions. As observed in the autoradiogram shown in Figure 5, the Pf92 HABP 33680 cross-linked to five RBC membrane proteins with apparent molecular weights of 68, 78, 85, 47, and 170 kDa under total binding conditions (Figure 5, lane 1), the two latter bands also being detected when the assay was carried out under unspecific binding conditions (Figure 5, lane 2). Therefore, the three bands recognized under total binding conditions but not under unspecific ones are likely to correspond to RBC receptors to which HABP 33680 binds specifically (Figure 5). Interestingly, bands of about 85 and 78 kDa were also recognized specifically but weakly by Pf113 HABPs 33723, 33728, 33740, 33745, 33748, and 33749 (data not shown).

Structural Features of Pf92 and Pf113 HABPs. The secondary structure elements of Pf92 and Pf113 HABPs were studied by circular dichroism (CD) spectroscopy. CD spectra showed α -helical features in Pf92 HABPs 33672 and 33677 as well as in all Pf113 HABPs, as indicated by the first molar ellipticity minimum between 204 and 208 nm and a second smaller minimum between 221 and 223 nm (Figure 6), which differed slightly from the characteristic minima of α -helical structures detected at 209 and 222 nm possibly

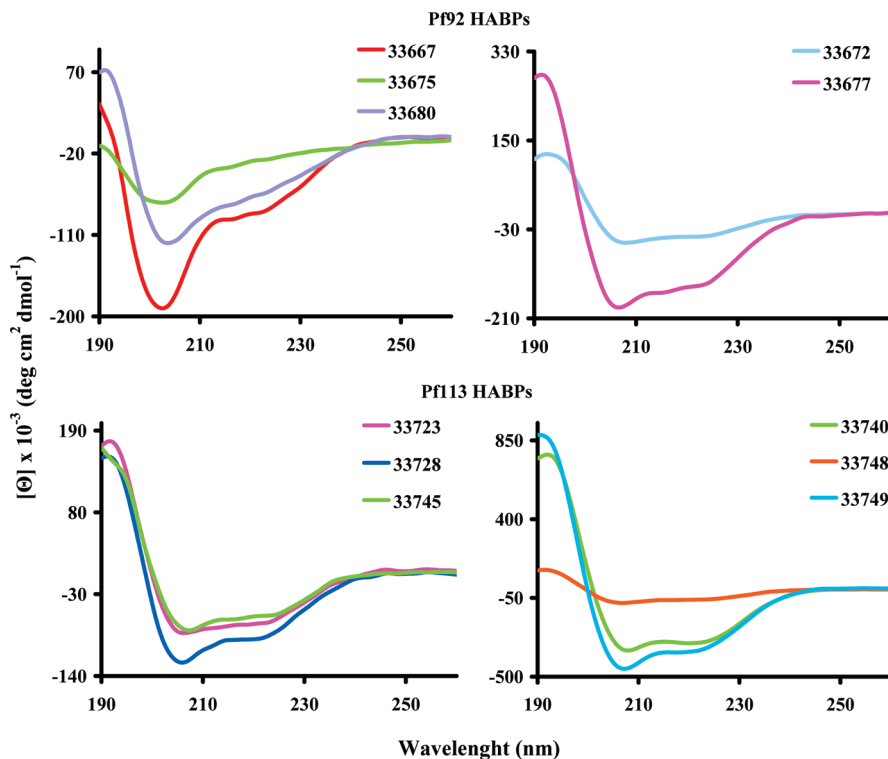


Figure 6. Circular dichroism spectra of Pf92 and Pf113 HABPs registered in 30% TFE.

because of the presence of other structural features in these HABPs. Data analysis with CDpro software showed a predominant α -helical content in Pf92 HABPs 33672 and 33677 as well as in Pf113 HABPs 33723, 33728, 33740, 33745, 33748, and 33749 (α -helical percentages ranged between 70% and 99% in all cases).

On the other hand, one ellipticity minimum at 201 nm and one ellipticity maximum between 210 and 212 nm were observed in the spectra of Pf92 HABPs 33667, 33675, and 33680, which is close to the characteristic minimum at 195 nm and maximum at 212 nm shown by random coil structures. Deconvolution indicated predominant random structures for these HABPs (40%) with a lesser content of other secondary structures.

DNA Amplification and Strain-Specific Polymorphism Analysis. The genetic fragments encoding Pf92 and Pf113 HABPs in the *P. falciparum* FCB-2, FVO, and PAS-2 strains were obtained from purified PCR products. Single bands of about 880 bp, 705 bp, 488 bp, and 772 bp were amplified using the four primer sets specified in the Experimental Section (Figure S2). These molecular weights agreed with the ones predicted on the basis of sequence. A single band of about 438 bp was amplified using the control primers (Figure S2).

The amino acid sequences of such gene fragments were aligned to the sequences of the 3D7, HB3, and Dd2 reference strains using Clustal W software.^{30,31} This analysis showed a 100% of identity among Pf92 HABPs 33667, 33672, 33675, and 33680 and among Pf113 HABPs 33723, 33728, 33740, 33745, 33748, and 33749 in the six *P. falciparum* strains (Figure S3). Non-synonymous nucleotide substitutions were observed among the aligned nucleotide sequences, as follows (Figure S3): A substitution from T to A was observed in nucleotide position 1278 of HABP 33677 (according to the 3D7 strain numbering) corresponding to the Pf92 amino acid position 426, where triplet AAT encodes for asparagine (N) in 3D7, FCB-2, FVO, PAS-2, and Dd2, while triplet AAA encodes for lysine (K) in HB3 (Figure S3A). This amino acid substitution was the only difference found among Pf92 HABPs' sequences.

Three additional strain-specific polymorphisms were found outside the region encoding Pf92 HABPs: a substitution from A to C in nucleotide position 1091 corresponding to residue 364, where triplet AAA encodes for lysine (K) in 3D7 while triplet ACA encodes for threonine (T) in the remaining strains (Figure S3A); a substitution from G to C in nucleotide position 1138 corresponding to residue 380, where triplet GCG encodes for alanine (A) in HB3 and 3D7 while triplet CCG encodes for proline (P) in the FCB-2, Dd2, FVO, and PAS-2 strains (Figure S3A); a substitution from G to A in nucleotide position 1633 of the 3D7 strain (amino acid 545), where triplet GAA encodes for glutamic acid (E) in the 3D7, FCB-2, FVO, PAS-2, and Dd2 strains while the triplet AAA encodes for lysine (K) in the HB3 strain (Figure S3B).

In Pf113, a single substitution was observed outside the region encoding HABPs, which consisted of a substitution from G to A in nucleotide position 1483 of the 3D7 strain corresponding to residue 495 where the GAT triplet encoding for aspartic acid (D) in 3D7, HB3, FCB-2, FVO, and PAS-2 is replaced in the Dd2 strain by the AAT triplet encoding for asparagine (N) (Figure S3D).

Invasion Inhibition Assays. All Pf92 and Pf113 HABPs had a moderate ability to inhibit *P. falciparum* invasion of uninfected RBCs, and such inhibition ability increased as the peptide concentration increased (Table 3), thereby

Table 3. Invasion Inhibition Assays (%)^a

	HABPs ^b		Antisera ^c		
	100 μ M	200 μ M	1:8	1:4	1:2
	Pf92				
33675	13	45			
33677	8	37			
33680	-3	76			
m-1			ND	ND	ND
33667	9	34			
33672	9	49			
m-2			50	83	93
33660 (<1:100) ^d					
33684 (1:6400) ^d					
33691 (1:6400) ^d					
	Pf113				
33740	8	40			
33745	15	47			
33748	7	42			
33749	11	37			
m-3			53	87	96
33723 (>1:12800) ^d	10	40			
33728 (>1:12800) ^d	4	36			
m-4			ND	ND	ND
	Controls				
Chloroquine (1.85 mg/mL)			81		
EGTA (1.9 mg/mL)			68		

^aStandard deviation were below 5%. ^bHABPs were used at two different concentrations. ^cSera were used at three dilutions. ^dAntibody titers are shown in brackets for each peptide in the inoculated mixture. ND: no data available.

suggesting that binding of Pf92 and Pf113 HABPs to RBCs could inhibit binding of native Pf92 and Pf113, as well as of other parasite proteins using the same RBC receptors. Interestingly, a stronger invasion inhibition ability was observed with rabbit polyclonal anti-m-2 and anti-m-3 sera (raised against Pf92 and Pf113 peptides, respectively), which also showed a concentration-dependent behavior (Table 3).

Discussion and Conclusions

A deeper understanding of molecular interactions between parasite proteins and RBC receptors can provide important clues for finding candidates to design an effective antimalarial vaccine.²⁷ The first indication that Pf92 and Pf113 could be interacting with RBC surface receptors during RBC invasion by *P. falciparum* merozoites is the localization of these proteins on the merozoite surface. In the present study, the localization of these proteins was assessed in *P. falciparum* intraerythrocytic stages by IFA, detecting Pf92 on the merozoite surface as well as in ring stages (Figure 3, panels B–I). This is interesting given that the transcriptome analysis suggests that Pf92 is only expressed in schizont stages,²³ and the GFP-Pf92 fusion protein fluorescence pattern indicates its localization in the merozoite surface but not in ring stages.⁸ Similarly, Pf113 was detected in this study in merozoite surface for the first time but not in ring stages (Figure 3, panels J–M), which differs from transcriptome studies showing the expression of this protein during schizonts and ring stages too.²³

Interestingly, the same rabbit polyclonal anti-Pf92 antiserum used in IFA studies strongly inhibited *P. falciparum* invasion of RBCs (Table 3) and recognized the complete Pf92 protein plus two apparent cleavage fragments in Western blot assays with parasite lysates, which suggests that Pf92 or regions from

this protein are internalized into the newly invaded RBC and that these regions remain bound to the ring stage. A similar behavior has been reported for the 19 kDa fragment of the leading vaccine candidate and major GPI-anchored protein MSP1, which is the only MSP1 portion dragged into newly invaded RBCs and against which monoclonal and polyclonal antibodies capable of partially or completely inhibiting *P. falciparum* invasion of RBCs have been raised.^{18,32} Similar to Pf92, the same rabbit polyclonal anti-Pf113 sera assessed in IFA studies recognized the complete protein together with two cleavage fragments in parasite protein lysate and strongly inhibited *P. falciparum* invasion of RBCs, therefore outlining the importance of Pf92 and Pf113 as merozoite ligands during RBC invasion.

Previous studies have suggested that Pf92 and Pf113 could be participating in the formation of a macromolecular complex in the merozoite surface, since both proteins are attached to the parasite membrane via GPI anchors.^{8,14,22} Particularly in the case of Pf113, its association with other unknown proteins has been suggested by blue native PAGE assays in which Pf113 peptides have been detected at higher molecular weight gel slices (>400 kDa) than the 113 kDa molecular weight predicted for this protein.¹⁴ Thus, Pf92 and Pf113 might be behaving as MSP1, which also undergoes several proteolytic cleavages and whose fragments associate with soluble fragments of MSP6, MSP7, and MSP9 to form a coligand complex that interacts with the band 3 protein of the RBC membrane.^{17,18}

We identified HABPs in both proteins, most of which bind with high affinity and positive cooperativity to noninfected human RBCs (Table 1), whereas others such as Pf113 HABPs 33740 and 33745 had higher K_d values and therefore are likely to establish specific but low affinity interactions with RBCs. These data suggest that Pf92 and Pf113 establish an array of specific binding interactions with RBC membrane receptors mediated through the HABPs herein identified, which are probably implicated in the parasite's rolling over RBC membrane and establishing multiple points of contact with the target cell, considering that it has been extensively reviewed that the merozoite uses high-affinity and low-affinity molecular interactions during the invasion process.¹⁶

In particular, Pf113 HABPs 33745 and 33749 showed a large number of binding sites per RBC but none of the RBC membrane proteins is known to be expressed in such a large amount. Furthermore, since these two HABPs cross-link to two RBC membrane proteins, it is reasonable to suggest that these two Pf113 regions have more than one binding site on RBC surface. In fact, the highest concentration of radiolabeled peptide used in saturation assays was not sufficient to occupy all receptors sites of HABP 33745 (Figure 4), which would correlate with this HABP's binding profile to enzyme-treated RBCs showing sensitivity to all enzymatic treatments (as discussed further below). Alternatively, since the number of binding sites for HABP 33749 was only slightly smaller than for HABP 33745 but they were saturable under the assessed conditions, binding sites for 33745 are probably saturable at a concentration larger than the ones assessed in this study.

Regarding the ability of Pf92/Pf113 HABPs to inhibit invasion of RBCs by *P. falciparum* merozoites, the results showed that HABPs behave in general as moderate inhibitors but none are able to completely inhibit RBC invasion (Table 3). The same behavior has been reported for the HABPs identified in the Cys₆ proteins Pf12, Pf38, and Pf41 as well as for HABPs derived from MSP1,^{21,25} which led to the

conclusion that invasion of RBCs cannot be completely inhibited by a single Pf92/Pf113 HABP but rather by a combination of HABPs derived from different merozoite proteins, since the analysis of *P. falciparum* transcriptome suggests that around 58–90 proteins are implicated in the different pathways used by the parasite to invade RBCs.^{23,33}

On the other hand, polyclonal anti-Pf92 and anti-Pf113 sera did have a strong inhibitory effect on merozoite invasion of RBCs, probably due to the following three steric hindrance effects. (1) Antibodies in these sera could have inhibited binding of native Pf92 and Pf113 to their RBC receptors. (2) Antibodies could have prevented binding of neighbor proteins (possibly involved in hypothetical Pf92/Pf113 complexes) to their receptor sites, and/or (3) antibodies could have hampered the formation of such Pf92/Pf113 complexes and thus affected their functioning.

The localization of HABPs in the amino acid sequences of Pf92 and Pf113 also provided interesting clues about the roles of these HABPs in merozoite invasion. Some Pf92/Pf113 HABPs were located in Cys-rich regions but not in the Pfs48/45 domain that has been described to participate in molecular interactions between RBC receptors and Cys₆ proteins (Figure 2), therefore suggesting the implication of these regions in parasite binding to RBCs, since previous studies have identified HABPs in other Cys-rich regions, such as the epidermal growth factor (EGF)-like and Duffy-binding-like (DBL) domains known to interact with host-cell surface receptors during merozoite invasion.^{16,34,35} It is therefore likely that Pf92 and Pf113 Cys-rich regions are involved in the formation of molecular structures different from the Pfs48/45 loops but also implicated in molecular interactions with RBC receptors.²¹

Interestingly, Pf92 HABPs 33667, 33675, and 33680 localized outside the Pfs48/45 domain but inside the cysteine-rich region showed high percentages of β -turn and unordered structures, same as has been reported for HABPs identified inside EGF-like domains of the GPI-anchored proteins MSP1, MSP2, MSP8, and MSP10,³⁶ whereas the remaining Pf92 and Pf113 HABPs showed high percentages of α -helical structure. This is relevant because it has been reported that the presentation of a HABP and its modified analogues by human leukocyte antigen (HLA) molecules/MHC II is directly correlated to the structure of both molecules.^{27,37,38} CD studies and nuclear magnetic resonance (¹H NMR) analysis of HABPs identified in several merozoite proteins, and HLA molecules have shown that peptides with α -helical structures bind with high affinity to HLA-DR52 molecules, whereas peptides with turn or unordered structures interact with HLA-DR53 molecules.³⁶ All this would be in agreement with the structural, functional, and immunological compartmentalization reported for *P. falciparum* proteins involved in invasion of host cells.³⁶

Once HABPs were identified and their potential biological importance was examined, the RBC membrane receptor for each HABP was evaluated by determining their susceptibility to different enzymatic treatments and assessing the apparent molecular weights of RBC membrane proteins cross-linked by some HABPs. As shown in Table 2, specific binding of most Pf92/Pf113 HABPs (Pf92 HABPs, 33667, 33672, 33675, and 33677; Pf113 HABPs 33723, 33728, 33740, 33748, and 33749) was drastically reduced by treating RBCs with neuraminidase, which suggests interaction with glycosylated receptors. This enzymatic susceptibility agrees with the sensitivity profile reported for glycophorins A, B, C or the unknown receptor

“E”;³³ however, none of the apparent molecular weights determined for the products cross-linked by the aforementioned HABPs agreed with the molecular weights of known glycoporphins, thereby suggesting binding to other sialic acid glycosylated receptors not yet characterized.

It is worth noting that the Pf92 HABP 33680, whose binding was resistant to neuraminidase, recognized specifically two bands (85 and 78 kDa, Figure 5) at the same molecular weights as the two bands recognized by all Pf113 HABPs (data not shown). Moreover, binding of Pf92 HABP 33680 was significantly diminished by treating RBCs with trypsin and slightly reduced by chymotrypsin, an enzymatic susceptibility profile also shown by the non-sialic acid glycosylated band 3 protein which has a molecular weight of ~90 kDa³⁹ that is close to the molecular weight of one of the RBC membrane proteins cross-linked by this HABP (85 kDa, Figure 5).

On the other hand, binding of Pf113 HABP 33745 was slightly affected by neuraminidase (<50% binding reduction) but more drastically by chymotrypsin and trypsin. It is therefore probable that this HABP is binding to glycosylated as well as to nonglycosylated receptors, since sensitivity to these three enzymatic treatments has not been reported for any known or unknown RBC surface receptor so far, and neither has an RBC receptor sensitive to chymotrypsin and trypsin been described yet.

It has been established that *P. falciparum* uses both sialic acid dependent and sialic acid independent pathways as routes for RBC invasion and that it changes from one invasion pathway to the other by switching on or off the expression of specific invasion ligands, which provides parasites with a variety of invasion phenotypes.³³ Because of the parasite's vast antigenic variability, a fully effective antimalarial vaccine against all *P. falciparum* strains should contain a large number of protein subunits conserved among all or almost all *P. falciparum* strains in order to reduce the parasite's ability to evade the host's immune response, whether it be by using alternative invasion pathways or inducing strain-restricted immune responses.^{27,40} For this reason, the polymorphism of Pf92 and Pf113 HABPs was analyzed in parasite strains isolated from different geographical regions, finding a single amino acid substitution in Pf113 HABP 33677. These data indicate that the Pf92 and Pf113 HABPs are highly conserved among parasite strains probably because of their involvement in processes important for parasite survival.

However, it has been reported that conserved HABPs should be specifically modified in order to be rendered into immunogenic protection inducers.^{27,37,38,41} Such poor immunogenicity of conserved HABPs could explain the low antibody production elicited by conserved HABPs Pf92 33667 and 33672, as indicated by the nonrecognition of any *P. falciparum* protein in Western blot and IFA studies. Interestingly, antibody titers elicited by Pf113 HABPs (33723 and 33728) were high (Table 3) despite being conserved, probably because of the use of the FIS peptide as antibody-production enhancer, which is a MHC II presentable T helper peptide known for rendering nonimmunogenic peptides into immunogenic and immunogenic peptides into even more stronger immunogenic.²⁸

Additionally, we observed that the use of the FIS peptide did not potentiate the immunogenicity of some of the peptides being inoculated into rabbits (m-1, m-4, and the Pf92 peptide 33660 from m-2; see Table 3), which is consistent with studies by Prieto et al.²⁸ On the other hand, given that peptides were

inoculated as mixtures (two or three peptides per mixture plus the FIS peptide), an inhibitory competition effect between these peptides for binding to the MHC II molecule cannot be ruled out nor can the existence of a preferential peptide presentation by MHC II molecules to T lymphocytes, as has been proposed by Prieto et al.²⁸ The above suggests that the concentration and immunogenic characteristics of each peptide are determinants for inducing or not inducing antibody production.

Curiously, the anti-m-3 sera raised against Pf113 HABPs 33723 and 33728 showed weak recognition of Pf113 by Western blot, even though high antibody titers against these two peptides were found in such sera by ELISA (Table 3). In addition, the same sera recognized the native protein in mature schizonts in IFA studies using high serum concentrations (1:5 dilution), compared to the serum concentrations used in IFA studies with other parasite proteins (1:20, 1:40, or even 1:160).^{27,38} This suggests the existence of a low number of Pf113 copies in the membrane of *P. falciparum* merozoites (FCB-2 strain), which would be in agreement with studies by Gilson et al. where 11 GPI-anchored proteins representing about 94% of the proteome of GPI-anchored proteins were stoichiometrically identified in *P. falciparum* schizonts (3D7 strain), but Pf113 was not detected probably because this protein is more broadly expressed in blood parasite stages (ring, trophozoites, and schizonts), as pointed out by the transcriptome.^{22,23}

Our findings corroborate the importance of DRM proteins in receptor–ligand interactions established between the parasite and its target cell during the invasion processes and highlight how such interactions could be mediated by sequences with defined structural elements. Bearing in mind all the results discussed in this study, the inclusion of HABPs derived from Pf92 and Pf113 in a vaccine, as well as HABPs derived from soluble proteins associated with these two GPI-anchored proteins, would be advisable, even more considering that Pf92 and Pf113 might be important for sorting of such soluble proteins to merozoite membrane.

Previous studies have shown that conserved HABPs do not induce a protective immune response in *Aotus* monkeys. However, a proper replacement of those residues that are critical for binding of HABPs to host cells by amino acids with similar mass but opposite polarity has been shown to improve their fitting inside MHC II (HLAs) and presentation to the TCR, therefore rendering conserved immunologically silent HABPs into immunogenic protection inducers.^{27,37,38,41} Further studies are needed in order to evaluate antibody production and protection induced by Pf92 and Pf113 HABPs and their analogues, and hence determine whether or not they should be included in a subunit antimalarial vaccine.

Experimental Section

Peptide Synthesis. The amino acid sequences of Pf92 (PF13_0338) and Pf113 (PF14_0201) were downloaded from the *P. falciparum* 3D7 genome database (available at www.plasmodb.org) and divided into 40 and 49 nonoverlapping 20-mer-long peptides, respectively, as shown in Figure 2. These peptides were synthesized using solid-phase multiple peptide synthesis,^{42,43} 4-methylbenzhydrylamine hydrochloride resin (0.5 mequiv/g), and *t*-Boc protected amino acids (Bachem). A tyrosine (Y) residue was added at the carboxyl terminus of those peptides not containing such residue in their sequence to enable ¹²⁵I-radiolabeling, and peptides were cleaved using the low–high hydrogen fluoride cleavage.⁴⁴ Peptides with ≥95% of

purity were obtained by combining analytical reversed-phase high-performance liquid chromatography (RP-HPLC), semipreparative RP-HPLC, and matrix assisted laser desorption/ionization time-of-flight mass spectrometry (MALDI-ToF MS) (Bruker Daltonics). Peptides were numbered according to our institute's serial system.

Radiolabeling. Peptides were radiolabeled according to a protocol described elsewhere.^{45,46} Briefly, an amount of 7 μ L of 2.6 mM peptide dissolved in 4-(2-hydroxyethyl)-1-piperazineethanesulfonic acid (HEPES) buffered saline (HBS) (0.01 M HEPES, 0.15 M NaCl, pH 7.4) was incubated for 15 min with 15 μ L of chloramine T (2.75 mg/mL) and 4 μ L of Na¹²⁵I (100 mCi/mL specific activity; MP Biomedicals). The reaction was stopped after 15 min by adding 15 μ L of sodium metabisulfite (2.25 mg/mL), and radiolabeled peptides were purified on a Sephadex G-10 column (10 mm \times 5 mm; Pharmacia, Uppsala, Sweden). Peptide radioactivity was determined on a γ counter (Auto Gamma Counter Cobra II, Packard).

Binding Assays. RBCs obtained from healthy donors were washed several times with HBS and centrifuged at 1500g for 5 min to remove white blood cells and plasma. To determine peptide specific binding, 1×10^8 RBCs were incubated for 90 min with increasing concentrations of radiolabeled peptide (0–570 nM) in the absence (total binding) or presence (unspecific binding) of an excess of unlabeled peptide (20 μ M), in a final volume of 200 μ L. Unbound peptide was removed by washing RBCs twice with HBS. RBC-associated radioactivity was determined in a γ counter. Peptides whose specific binding plots (specific binding = total binding – nonspecific binding) showed a slope equal to or greater than 0.02 ($\geq 2.0\%$ specific binding) were considered as HABPs given that binding activity is related to the ratio between radiolabeled peptide specifically bound to RBCs and added radiolabeled peptide.^{16,25} Assays were performed in triplicate.

As assay specificity control, binding assays were carry out using scrambled-sequence peptides from Pf92 HABPs 33667 and 33675 and scrambled-sequence peptides from Pf113 HABPs 33723, 33740, and 33748; all these peptides had the same amino acid composition of their corresponding HABPs but random sequence order.

Production of Anti-Pf92 and Anti-Pf113 Sera. Two New Zealand rabbits nonreactive to *P. falciparum* lysates (as determined by Western blot) were subcutaneously inoculated with 1 mg/mL of mixtures containing equal amounts of each Pf92 and Pf113 peptide and 1 mg/mL of the T-helper cell determinant peptide (FIS, ¹⁰⁶FISEAIIHVLHSR¹¹⁸) from sperm whale.²⁸ Mixture 1 (m-1) contained Pf92 HABPs 33667, 33672 and FIS; m-2 consisted of the Pf92 peptides 33660, 33684, 33691, and FIS; m-3 contained Pf113 HABPs 33723, 33728 and FIS; m-4 contained Pf113 peptides 33733, 33754, 33765, and FIS (Table 3). All these Pf92/Pf113 peptides, except for Pf113 33728, corresponded to B-cell epitopes predicted using the BepiPred 1.0 prediction server.⁴⁷ Two animals were inoculated per peptide mixture, the other two were inoculated only with FIS. Freund's complete adjuvant was used for the first dose (day 0), and Freund's incomplete adjuvant was used for the second and third doses (administered on days 20 and 40, respectively). Rabbit serum samples were collected on days 0 (preimmune), 20 (post-I), 40 (post-II), and 60 (post-III, final bleeding) to assess antibody production. Animals were handled in accordance to the guidelines of the Colombian Ministry of Public Health for handling research animals.

Nonspecific antibodies were removed by absorbing serum samples on *Escherichia coli* and *Mycobacterium smegmatis* lysates and SPf66 vaccine peptides, individually coupled to CNBr-activated Sepharose 4B (Pharmacia Biotech), as described elsewhere.^{48,49} Briefly, each serum sample (5 mL) was added to lysate-coupled Sepharose affinity columns (5 mL) and left under gentle shaking for 30 min at room temperature. This procedure was done twice using a new lysate-coupled Sepharose

affinity column each time. Purified antisera were stored at -70°C until use.

SDS-PAGE and Western Blot. The reactivity of purified anti-Pf92 and anti-Pf113 sera against a lysate of mature *P. falciparum* schizonts (FCB-2 strain) was tested by Western blot. Briefly, 500 μ g/mL of lysate were electrophoretically separated by sodium dodecyl sulfate–polyacrylamide gel electrophoresis (SDS–PAGE) in a discontinuous 7.5–15% (w/v) acrylamide gel gradient and transferred to nitrocellulose membrane (Hybond 203c, Pharmacia) by the semidry blotting technique. The nitrocellulose membrane was blocked for 1 h with 5% skimmed milk diluted in Tris-buffered saline–0.05% Tween (TBS–T) and then washed thrice with TBS–T. Preimmune and final bleeding serum samples diluted 1:100 in 5% skimmed milk–TBS–T were individually incubated with a membrane strip. After five washes with TBS–T, strips were incubated for 1 h with 1:5000 alkaline phosphatase-conjugated antirabbit IgG antibodies (ICN Biomedicals). The immunoreaction was detected using NBT/BCIP (KPL, Gaithersburg). Sera from rabbits inoculated only with FIS were assessed as control.

IFA Studies. Mature schizonts and ring stages were obtained from a synchronized continuous culture of the *P. falciparum* FCB-2 strain maintained as described elsewhere.^{50,51} Culture samples (10% parasitemia) were washed with sterile phosphate buffered saline (PBS) containing 0.15 M NaCl, pH 7.2, suspended in fetal bovine serum (FBS)–PBS (1:1, v/v), seeded on glass slides and left to air-dry. Slides were blocked for 10 min with 1% skimmed milk and incubated for 30 min with preimmune or post-III purified serum samples using a 1:5 dilution of purified antirabbit IgG-FITC conjugate F(ab)₂ fragment as secondary antibody (Vector Laboratories Inc.).⁵² Preimmune rabbit sera were used as negative controls. Immunofluorescence was visualized on an Olympus BX51 fluorescence microscope. Sera from rabbits inoculated only with FIS were assessed as control.

ELISA. Rabbits' sera that detected parasite proteins in Western blot and IFA studies (i.e., sera raised against m-2 and m-3) were assessed by ELISA to detect total IgG against each individual peptide as described elsewhere.⁵³ Briefly, 2-fold serum serial dilutions were obtained from a 1:100 sera dilution in PBS–0.5% Tween and 5% skimmed milk. Peptides (10 μ g/mL) previously preabsorbed onto 96-well plates were incubated with serum dilutions for 1 h at 37 $^\circ\text{C}$. Plates were then washed 5 times with PBS–Tween 0.5% and left to air-dry before adding peroxidase-conjugated antirabbit IgG diluted 1:5000 in PBS–0.5% Tween and 5% skimmed milk. After the plates were incubated for 1 h, they were washed 5 times and the formation of antigen–antibody complexes was detected using the TMB Microwell peroxidase substrate system kit (KPL Laboratories). Absorbance was measured at 620 nm using a microtiter reader (Labsystems Multiskan MS).

HABP Saturation Assays. Saturation assays were carried out with Pf92 and Pf113 HABPs as described elsewhere.^{45,46} In brief, 7.5×10^7 RBCs were incubated for 90 min with increasing concentrations of ¹²⁵I-labeled peptide in the presence (unspecific binding) or absence (total binding) of unlabeled peptide (24 μ M). Unbound ligand was removed by washing RBCs twice with HBS, and RBC-associated radioactivity was measured with a γ counter (Auto Gamma Counter Cobra II, Packard). All assays were performed in triplicate. Binding data were plotted to obtain dissociation constants (K_d) and Hill coefficients (n_H).²⁵

Binding Assays with Enzyme-Treated RBCs. RBCs suspended in HBS (60% hematocrit) were incubated for 60 min at 37 $^\circ\text{C}$ with ~ 150 μ U/mL neuraminidase (ICN 9001-67-6) or with either 1 mg/mL trypsin (Sigma T-1005) or 1 mg/mL chymotrypsin (Sigma C-4129). Binding of HABPs to enzyme-treated RBCs (1×10^8 cells/ μ L) was assessed in triplicate as described above in binding assays. Binding to untreated RBCs was considered as positive control (100% specific binding).²⁵

Cross-Linking Assays. RBC suspensions (5×10^7 cells) were incubated for 90 min with radiolabeled HABPs in the absence (total binding) or presence of nonradiolabeled peptide (unspecific binding). Bound HABPs were cross-linked to RBC receptors by incubation with 100 μ L of bis-sulfosuccinimidyl suberate (BS³, 1 mg/mL) for 1 h at room temperature, stopping the reaction by addition of Tris-HCl buffer. Samples were pelleted by centrifugation at 1500g for 5 min and then incubated for 1 h with 15 μ L of lysis buffer (5 mM Tris-HCl, 7 mM NaCl, 1 mM ethylenediaminetetraacetic acid, 0.1 mM phenylmethylsulfonyl fluoride) plus 15 μ L of Laemmli buffer. Samples were then centrifuged at 1700g for 15 min and separated by 12% SDS-PAGE. The resulting gel was exposed to radiation-sensitive film and the autoradiogram was revealed after 15–20 days. Apparent molecular weights of proteins were determined using molecular weight markers (Bio Labs).

Merozoite Invasion Inhibition Assays. *P. falciparum* parasite cultures (FCB-2 strain) synchronized at the schizont stage were seeded in 96-well plates (5% hematocrit and 5% parasitemia) and incubated with unlabeled HAPB (100 and 200 μ M) or rabbit anti-m-2 or anti-m-3 sera (1:2, 1:4 and 1:8 dilutions). After 18 h of incubation at 37 °C under a 5% O₂, 5% CO₂, and 90% N₂ atmosphere, the supernatant was discarded and cells were labeled by incubation at 37 °C for 30 min with 15 μ g/mL hydroethidine, washed, and analyzed in a FACS Calibur flow cytometer (FACSort, FL2 channel) equipped with CellQuest software.⁵⁴ Controls included infected and uninfected RBCs treated with either ethylene glycol tetraacetic acid (EGTA) or chloroquine.

Circular Dichroism Analysis. The secondary structure elements of Pf92 and Pf113 HABPs were examined by CD spectroscopy. Briefly, 5 μ M peptide solutions in 30% (v/v) 2,2,2-trifluoroethanol (TFE)–water were measured in a Jasco J810 CD spectrometer using a nitrogen-flushed 1 cm path-length cuvette. Each spectrum was obtained by averaging three scans taken at room temperature over a wavelength range of 190–260 nm, with a 20 nm/min scan rate and 1 nm spectral bandwidth (corrected for baseline values). Data were processed using the Spectra Manager software CD spectra, which is equipped with SELCON3, CONTINLL, and CDSSTR deconvolution programs.^{55,56}

DNA Extraction and Purification. Genomic DNA (gDNA) was obtained from in vitro cultures of the *P. falciparum* FCB-2 (Colombian), FVO (Vietnamese), and PAS-2 (unknown origin) strains maintained as described elsewhere.^{50,51} In brief, parasitized RBCs (30% parasitemia) were lysed using 0.2% saponin and gDNA was purified using the UltraClean DNA blood isolation kit (MO BIO, Carlsbad).

PCR Amplification. The sequences of the Pf92 (PF13_0338) and Pf113 (PF14_0201) genes reported for the 3D7 reference strain were analyzed using Gene Runner, version 3.05, in order to design primers to amplify Pf92 and Pf113 HABPs. The following four primer sets were designed: (1) Pf92-f1 (5'-AGACCAGGAATATATGAGAG-3') and Pf92-r1 (5'-ACTCAAGACAATACGTAC-3') amplifying the region encoding HABPs 33667, 33672, 33675, and 33677; (2) Pf92-f2 (5'-GTACGTATTGTGCTTGAGT-3') and Pf92-r2 (5'-TGATTACAT-TATTATTAACATTAC-3') amplifying the region encoding HAPB 33680; (3) Pf113-f1 (5'-ATGGGAATAACGAGATAA-TAC-3') and Pf113-r1 (5'-CATACAACATTAACAGACAC-3') amplifying the region encoding HABPs 33723 and 33728; (4) Pf113-f2 (5'-CGTGATGCAAATCCAGATG-3') and Pf113-r2 (5'-ATACAGCCATTCTTATCG-3') amplifying the region encoding HABPs 33740, 33745, 33748, and 33749. The DIR1/REV1 primers amplifying the region encoding HAPB 33577 of the *P. falciparum* integral membrane protein Pf25-IMP were used as PCR positive control.⁵²

The PCR mix (50 μ L) contained the following reagents: 2 μ L of isolated *P. falciparum* gDNA (FCB-2, FVO, or PAS-2), 1 U of Taq polymerase (Bioline, Taunton, MA), 1 \times Taq polymerase reaction buffer, 1.5 mM MgCl₂, 0.2 mM dNTPs, and 0.4 μ M of

each primer. Thermocycling conditions were as follows: initial denaturation at 95 °C for 5 min followed by 35 cycles of 1 min annealing at 56 °C for Pf92-f1/Pf92-r1, Pf92-f2/Pf92-r2, Pf113-f1/Pf113-r1, and Pf113-f2/Pf113-r2 or at 58 °C for DIR1/REV1, 1 min extension at 72 °C, and 1 min denaturation at 95 °C; a final extension cycle was carried out at 72 °C for 5 min. Samples containing water instead of DNA were used as negative control. Amplification products were visualized on 1% agarose gels stained with SYBR safe (Invitrogen, Eugene), purified using the Wizard PCR preps kit (Promega, Madison), and sequenced using their corresponding forward and reverse primers.

Acknowledgment. Nora Martínez and Paula Juliana Martínez assisted in the translation and revision of this manuscript.

Supporting Information Available: Binding profile of scrambled-sequence HABPs, PCR amplification of the regions encoding HABPs in the Pf92 and Pf113 proteins, and amino acid sequence alignment of the regions encoding Pf92 and Pf113 HABPs in the *P. falciparum* 3D7, FCB-2, FVO, PAS-2, HB3, and Dd2 strains. This material is available free of charge via the Internet at <http://pubs.acs.org>.

References

- (1) Pralle, A.; Keller, P.; Florin, E. L.; Simons, K.; Horber, J. K. Sphingolipid-cholesterol rafts diffuse as small entities in the plasma membrane of mammalian cells. *J. Cell Biol.* **2000**, *148*, 997–1008.
- (2) Simons, K.; Ikonen, E. How cells handle cholesterol. *Science* **2000**, *290*, 1721–1726.
- (3) Zacharias, D. A.; Violin, J. D.; Newton, A. C.; Tsien, R. Y. Partitioning of lipid-modified monomeric GFPs into membrane microdomains of live cells. *Science* **2002**, *296*, 913–916.
- (4) Simons, K.; Ehehalt, R. Cholesterol, lipid rafts, and disease. *J. Clin. Invest.* **2002**, *110*, 597–603.
- (5) Brown, D. A.; London, E. Functions of lipid rafts in biological membranes. *Annu. Rev. Cell Dev. Biol.* **1998**, *14*, 111–136.
- (6) Simons, K.; Toomre, D. Lipid rafts and signal transduction. *Nat. Rev. Mol. Cell Biol.* **2000**, *1*, 31–39.
- (7) Mukherjee, S.; Maxfield, F. R. Role of membrane organization and membrane domains in endocytic lipid trafficking. *Traffic* **2000**, *1*, 203–211.
- (8) Sanders, P. R.; Gilson, P. R.; Cantin, G. T.; Greenbaum, D. C.; Nebl, T.; Carucci, D. J.; McConville, M. J.; Schofield, L.; Hodder, A. N.; Yates, J. R., 3rd; Crabb, B. S. Distinct protein classes including novel merozoite surface antigens in raft-like membranes of *Plasmodium falciparum*. *J. Biol. Chem.* **2005**, *280*, 40169–40176.
- (9) Cowman, A. F.; Crabb, B. S. Invasion of red blood cells by malaria parasites. *Cell* **2006**, *124*, 755–766.
- (10) Murphy, S. C.; Hiller, N. L.; Harrison, T.; Lomasney, J. W.; Mohandas, N.; Haldar, K. Lipid rafts and malaria parasite infection of erythrocytes. *Mol. Membr. Biol.* **2006**, *23*, 81–88.
- (11) Snow, R. W.; Guerra, C. A.; Noor, A. M.; Myint, H. Y.; Hay, S. I. The global distribution of clinical episodes of *Plasmodium falciparum* malaria. *Nature* **2005**, *434*, 214–217.
- (12) Mita, T.; Tanabe, K.; Takahashi, N.; Culletton, R.; Ndounga, M.; Dzodzomenyo, M.; Akhwale, W. S.; Kaneko, A.; Kobayakawa, T. Indigenous evolution of *Plasmodium falciparum* pyrimethamine resistance multiple times in Africa. *J. Antimicrob. Chemother.* **2008**, *63*, 252–255.
- (13) Wang, L.; Mohandas, N.; Thomas, A.; Coppel, R. L. Detection of detergent-resistant membranes in asexual blood-stage parasites of *Plasmodium falciparum*. *Mol. Biochem. Parasitol.* **2003**, *130*, 149–153.
- (14) Sanders, P. R.; Cantin, G. T.; Greenbaum, D. C.; Gilson, P. R.; Nebl, T.; Moritz, R. L.; Yates, J. R., 3rd; Hodder, A. N.; Crabb, B. S. Identification of protein complexes in detergent-resistant membranes of *Plasmodium falciparum* schizonts. *Mol. Biochem. Parasitol.* **2007**, *154*, 148–157.
- (15) Gaur, D.; Mayer, D. C.; Miller, L. H. Parasite ligand–host receptor interactions during invasion of erythrocytes by *Plasmodium* merozoites. *Int. J. Parasitol.* **2004**, *34*, 1413–1429.
- (16) Rodriguez, L. E.; Curtidor, H.; Urquiza, M.; Cifuentes, G.; Reyes, C.; Patarroyo, M. E. Intimate molecular interactions of *P. falciparum* merozoite proteins involved in invasion of red blood cells and their implications for vaccine design. *Chem. Rev.* **2008**, *108*, 3656–3705.

- (17) Li, X.; Chen, H.; Oo, T. H.; Daly, T. M.; Bergman, L. W.; Liu, S. C.; Chishti, A. H.; Oh, S. S. A co-ligand complex anchors *Plasmodium falciparum* merozoites to the erythrocyte invasion receptor band 3. *J. Biol. Chem.* **2004**, *279*, 5765–5771.
- (18) Kauth, C. W.; Woehlbier, U.; Kern, M.; Mekonnen, Z.; Lutz, R.; Mucke, N.; Langowski, J.; Bujard, H. Interactions between merozoite surface proteins 1, 6, and 7 of the malaria parasite *Plasmodium falciparum*. *J. Biol. Chem.* **2006**, *281*, 31517–31527.
- (19) Carter, R. Transmission blocking malaria vaccines. *Vaccine* **2001**, *19*, 2309–2314.
- (20) van Dijk, M. R.; Janse, C. J.; Thompson, J.; Waters, A. P.; Braks, J. A.; Dodemont, H. J.; Stunnenberg, H. G.; van Gemert, G. J.; Sauerwein, R. W.; Eling, W. A central role for P48/45 in malaria parasite male gamete fertility. *Cell* **2001**, *104*, 153–164.
- (21) Garcia, J.; Curtidor, H.; Pinzon, C. G.; Vanegas, M.; Moreno, A.; Patarroyo, M. E. Identification of conserved erythrocyte binding regions in members of the *Plasmodium falciparum* Cys(6) lipid raft-associated protein family. *Vaccine* **2009**, *27*, 3953–3962.
- (22) Gilson, P. R.; Nebl, T.; Vukcevic, D.; Moritz, R. L.; Sargeant, T.; Speed, T. P.; Schofield, L.; Crabb, B. S. Identification and stoichiometry of glycosylphosphatidylinositol-anchored membrane proteins of the human malaria parasite *Plasmodium falciparum*. *Mol. Cell. Proteomics* **2006**, *5*, 1286–1299.
- (23) Bozdech, Z.; Llinas, M.; Pulliam, B. L.; Wong, E. D.; Zhu, J.; DeRisi, J. L. The transcriptome of the intraerythrocytic developmental cycle of *Plasmodium falciparum*. *PLoS Biol.* **2003**, *1*, No. E5.
- (24) Ansari, F. A.; Kumar, N.; Bala Subramanyam, M.; Gnanamani, M.; Ramachandran, S. MAAP: malarial adhesins and adhesin-like proteins predictor. *Proteins* **2008**, *70*, 659–666.
- (25) Urquiza, M.; Rodriguez, L. E.; Suarez, J. E.; Guzman, F.; Ocampo, M.; Curtidor, H.; Segura, C.; Trujillo, E.; Patarroyo, M. E. Identification of *Plasmodium falciparum* MSP-1 peptides able to bind to human red blood cells. *Parasite Immunol.* **1996**, *18*, 515–526.
- (26) Rodriguez, L. E.; Urquiza, M.; Ocampo, M.; Suarez, J.; Curtidor, H.; Guzman, F.; Vargas, L. E.; Trivinos, M.; Rosas, M.; Patarroyo, M. E. *Plasmodium falciparum* EBA-175 kDa protein peptides which bind to human red blood cells. *Parasitology* **2000**, *120* (Part 3), 225–235.
- (27) Patarroyo, M. E.; Patarroyo, M. A. Emerging rules for subunit-based, multiantigenic, multistage chemically synthesized vaccines. *Acc. Chem. Res.* **2008**, *41*, 377–386.
- (28) Prieto, I.; Hervas-Stubbis, S.; Garcia-Granero, M.; Berasain, C.; Riezu-Boj, J. I.; Lasarte, J. J.; Sarobe, P.; Prieto, J.; Borrás-Cuesta, F. Simple strategy to induce antibodies of distinct specificity: application to the mapping of gp120 and inhibition of HIV-1 infectivity. *Eur. J. Immunol.* **1995**, *25*, 877–883.
- (29) Weber, J. L.; Lyon, J. A.; Wolff, R. H.; Hall, T.; Lowell, G. H.; Chulay, J. D. Primary structure of a *Plasmodium falciparum* malaria antigen located at the merozoite surface and within the parasitophorous vacuole. *J. Biol. Chem.* **1988**, *263*, 11421–11425.
- (30) Combet, C.; Blanchet, C.; Geourjon, C.; Deléage, G. NPS@: network protein sequence analysis. *Trends Biochem. Sci.* **2000**, *25*, 147–150.
- (31) Thompson, J. D.; Higgins, D. G.; Gibson, T. J. CLUSTAL W: improving the sensitivity of progressive multiple sequence alignment through sequence weighting, position-specific gap penalties and weight matrix choice. *Nucleic Acids Res.* **1994**, *22*, 4673–4680.
- (32) Blackman, M. J.; Heidrich, H. G.; Donachie, S.; McBride, J. S.; Holder, A. A. A single fragment of a malaria merozoite surface protein remains on the parasite during red cell invasion and is the target of invasion-inhibiting antibodies. *J. Exp. Med.* **1990**, *172*, 379–382.
- (33) Baum, J.; Maier, A. G.; Good, R. T.; Simpson, K. M.; Cowman, A. F. Invasion by *P. falciparum* merozoites suggests a hierarchy of molecular interactions. *PLoS Pathog.* **2005**, *1*, No. e37.
- (34) Sanders, P. R.; Kats, L. M.; Drew, D. R.; O'Donnell, R. A.; O'Neill, M.; Maier, A. G.; Coppel, R. L.; Crabb, B. S. A set of glycosylphosphatidyl inositol-anchored membrane proteins of *Plasmodium falciparum* is refractory to genetic deletion. *Infect. Immun.* **2006**, *74*, 4330–4338.
- (35) Michon, P.; Stevens, J. R.; Kaneko, O.; Adams, J. H. Evolutionary relationships of conserved cysteine-rich motifs in adhesive molecules of malaria parasites. *Mol. Biol. Evol.* **2002**, *19*, 1128–1142.
- (36) Reyes, C.; Patarroyo, M. E.; Vargas, L. E.; Rodriguez, L. E.; Patarroyo, M. A. Functional, structural, and immunological compartmentalisation of malaria invasive proteins. *Biochem. Biophys. Res. Commun.* **2007**, *354*, 363–371.
- (37) Cifuentes, G.; Patarroyo, M. E.; Urquiza, M.; Ramirez, L. E.; Reyes, C.; Rodriguez, R. Distorting malaria peptide backbone structure to enable fitting into MHC class II molecules renders modified peptides immunogenic and protective. *J. Med. Chem.* **2003**, *46*, 2250–2253.
- (38) Patarroyo, M. E.; Cifuentes, G.; Vargas, L. E.; Rosas, J. Structural modifications enable conserved peptides to fit into MHC molecules thus inducing protection against malaria. *ChemBioChem* **2004**, *5*, 1588–1593.
- (39) Yu, J.; Steck, T. L. Isolation and characterization of band 3, the predominant polypeptide of the human erythrocyte membrane. *J. Biol. Chem.* **1975**, *250*, 9170–9175.
- (40) Biggs, B. A.; Gooze, L.; Wycherley, K.; Wollish, W.; Southwell, B.; Leech, J. H.; Brown, G. V. Antigenic variation in *Plasmodium falciparum*. *Proc. Natl. Acad. Sci. U.S.A.* **1991**, *88*, 9171–9174.
- (41) Cifuentes, G.; Bermudez, A.; Rodriguez, R.; Patarroyo, M. A.; Patarroyo, M. E. Shifting the polarity of some critical residues in malarial peptides' binding to host cells is a key factor in breaking conserved antigens' code of silence. *Med. Chem.* **2008**, *4*, 278–292.
- (42) Houghten, R. A. General method for the rapid solid-phase synthesis of large numbers of peptides: specificity of antigen-antibody interaction at the level of individual amino acids. *Proc. Natl. Acad. Sci. U.S.A.* **1985**, *82*, 5131–5135.
- (43) Merrifield, R. B. Solid-phase peptide synthesis. I. The synthesis of a tetrapeptide. *J. Am. Chem. Soc.* **1963**, *85*, 2149–2154.
- (44) Tam, J. P.; Heath, W. F.; Merrifield, R. B. SN 1 and SN 2 mechanisms for the deprotection of synthetic peptides by hydrogen fluoride. Studies to minimize the tyrosine alkylation side reaction. *Int. J. Pept. Protein Res.* **1983**, *21*, 57–65.
- (45) Hulme, E. C. *Receptor-Ligand Interactions. A Practical Approach*; Oxford University Press, New York, 1993.
- (46) Yamamura, H. I.; Enna, S. J.; Kuhar, M. J. *Neurotransmitter Receptor Binding*; Raven Press: New York, 1978.
- (47) Larsen, J. E.; Lund, O.; Nielsen, M. Improved method for predicting linear B-cell epitopes. *Immunome Res.* **2006**, *2*, 2.
- (48) Patarroyo, M. E.; Romero, P.; Torres, M. L.; Clavijo, P.; Moreno, A.; Martinez, A.; Rodriguez, R.; Guzman, F.; Cabezas, E. Induction of protective immunity against experimental infection with malaria using synthetic peptides. *Nature* **1987**, *328*, 629–632.
- (49) Patarroyo, M. E.; Amador, R.; Clavijo, P.; Moreno, A.; Guzman, F.; Romero, P.; Tascon, R.; Franco, A.; Murillo, L. A.; Ponton, G.; et al. A synthetic vaccine protects humans against challenge with asexual blood stages of *Plasmodium falciparum* malaria. *Nature* **1988**, *332*, 158–161.
- (50) Lambros, C.; Vanderberg, J. P. Synchronization of *Plasmodium falciparum* erythrocytic stages in culture. *J. Parasitol.* **1979**, *65*, 418–420.
- (51) Trager, W.; Jensen, J. B. Cultivation of malarial parasites. *Nature* **1978**, *273*, 621–622.
- (52) Curtidor, H.; Arevalo, G.; Vanegas, M.; Vizcaino, C.; Patarroyo, M. A.; Forero, M.; Patarroyo, M. E. Characterization of *Plasmodium falciparum* integral membrane protein Pf25-IMP and identification of its red blood cell binding sequences inhibiting merozoite invasion in vitro. *Protein Sci.* **2008**, *17*, 1494–1504.
- (53) Druilhe, P.; Bouharoun-Tayoun, H. Human antibody subclass ELISA. *Methods Mol. Med.* **2002**, *72*, 457–459.
- (54) Wyatt, C. R.; Goff, W.; Davis, W. C. A flow cytometric method for assessing viability of intraerythrocytic hemoparasites. *J. Immunol. Methods* **1991**, *140*, 23–30.
- (55) Compton, L. A.; Johnson, W. C., Jr. Analysis of protein circular dichroism spectra for secondary structure using a simple matrix multiplication. *Anal. Biochem.* **1986**, *155*, 155–167.
- (56) Sreerama, N.; Venyaminov, S. Y.; Woody, R. W. Estimation of the number of alpha-helical and beta-strand segments in proteins using circular dichroism spectroscopy. *Protein Sci.* **1999**, *8*, 370–380.
- (57) Pinzon, C. G.; Curtidor, H.; Bermudez, A.; Forero, M.; Vanegas, M.; Rodriguez, J.; Patarroyo, M. E. Studies of *Plasmodium falciparum* rhoptry-associated membrane antigen (RAMA) protein peptides specifically binding to human RBC. *Vaccine* **2008**, *26*, 853–862.